Avrupa Bilim ve Teknoloji Dergisi
Sayı 19, S. 633-642, Ağustos 2020

Araştırma Makalesi

www.ejosat.com ISSN:2148-2683

European Journal of Science and Technology
No 19, pp. 633-642, August2020

Research Article

Microstructure and Chemical Analysis of Vehicle Brake Wear Particle Emissions

Bekir Güney[1*], Ali Öz[2]

[1] Karamanoglu MehmetbeyUniversity, Vocational School of Technical Sciences, Karaman, Türkiye (ORCID: 0000-0001-9764-9313)
[2]Mehmet Akif ErsoyUniversity, Vocational School of Technical Sciences, Burdur, Türkiye (ORCID: 0000-0002-0814-4020)

(First received 10 May 2020 and in final form 26 June 2020)

(**DOI:**10.31590/ejosat.744098)

ATIF/REFERENCE: Güney, B. & Öz, A. (2020). Microstructure and Chemical Analysis of Vehicle Brake Wear Particle Emissions. *European Journal of Science and Technology*, (19), 633-642.

Abstract

Vehicle emissions cause serious environmental problems, especially in industrial areas and populated areas. Although exhaust emissions are tried to be reduced by legal regulations, it is clear that non-exhaust emissions also increase significantly. Brake wear emissions are one of the most important sources of non-exhaust emissions. Brake wear particles are usually result from a cast-iron disc and a composite pad pair that is accompanied by friction. The chemical composition of these materials affects the content of the wear particles. The purpose of this study is to investigate the chemical and microstructural characterization of brake wear emission material of brake discs and pads commercially available to the market by Original Equipment Manufacturers (OEMs). Microstructure characterization of the wear particles was analyzed with field scanning electron microscopy (SEM); elemental analysis was conducted with energy dispersing spectrometer (EDS); crystal structures were analyzed with X-ray diffraction (XRD), and molecular bond structures were analyzed with the aid of fourier-transform infrared spectroscopy (FTIR). As a result of the analysis, it was found out that elements such as C, N, O, F, Si, Ca, Fe and Cu; sulfates, phosphates, oxides, and different mineral structures exist in the chemistry of wear particles. Especially, the presence of oxidized structures and heavy metals, pose a serious threat to human health and the environment. This study will provide important information for policymakers and researchers.

Keywords: Brake wear, Particulate matter, Emission, Environmental pollution, SEM, XRD, FTIR

Taşıt Freni Aşınma Parçacık Emisyonlarının Mikroyapısı ve Kimyasal Analizi

Öz

Taşıtlardan kaynaklanan emisyonlar özellikle endüstriyel alanlarda ve kalabalık nüfuslu yerlerde önemli çevre problemlerine sebep olmaktadır. Egzoz emisyonları yasal düzenlemelerle azaltılmaya çalışılsa bile egzoz dışı emisyonlar da hissedilir derecede artış olduğu açıktır. Fren aşıntı emisyonları egzoz dışı emisyonların en önemli kaynaklarından birisidir. Fren aşıntı partiküllerine genellikle dökme demir disk ve ona karşı sürtünme eşliği eden kompozit bir balata ikilisi kaynaklık eder. Bu malzemelerin kimyasal kompozisyonu aşıntı partiküllerinin içeriğine etki eder. Bu çalışma, Orijinal Ekipman Üreticileri (OEM) tarafından piyasaya ticari olarak sunulan fren disk ve balatalarına ait fren aşınma emisyon maddesinin kimyasal ve mikroyapısal karakterizasyonu araştırmak amacıyla yapılmıştır. Aşıntı partiküllerinin mikroyapı karekterizasyonu, alan taramalı elektron mikroskobu (SEM), elementel analizi enerji dağıtıcı spektrometre (EDS), kristal yapıları X-ray diffraction (XRD) ve moleküler bağ yapıları fourier dönüşümlü kızılötesi spektroskopisi (FTIR) cihazı yardımıyla analiz edildi. Analizler sonunda C, N, O, F, Si, Ca, Fe ve Cu gibi elementler, sülfatlar, fosfatlar, oksitler ve farklı mineral yapıların aşınma partikülleri kimyasında bulunduğu tespit edilmiştir. Bilhassa oksitli yapıların ve ağır metallerin varlığı insan sağlığı ve çevre açısından ciddi tehditler içermektedir. Bu çalışma politika yapıcılar ve araştırmacılar için önemli bilgiler sağlayacaktır.

Anahtar Kelimeler: Fren aşınması , Partikül madde, Emisyon, Çevre kirliliği, SEM, XRD, FTIR

[*]Corresponding Author: Karamanoglu Mehmetbey University, Vocational School of Technical Sciences, Karaman, Türkiye, ORCID: 0000-0001-9764-9313, guneyb@kmu.edu.tr

1. Introduction

Air pollution, that is increasing surprisingly, is one of the most critical problems caused by industrial civilization. Pollution has become an important issue as it negatively affects human health in many ways (Amato, 2018; Khodakarami, & Ghobadi, 2016). Strong correlations were found between intense pollution in the atmosphere and increased mortality due to asthma, lung cancer, cardiovascular disease, respiratory diseases, and skin diseases (Oberdörster et al., 2005; Pope Iii et al., 2002). Air pollutants are the heterogeneous mixture of many substances from different sources, with different physical and chemical conditions (Radhakrishnan, Devarajan, Mahalingam, & Nagappan, 2017).

The use of fossil fuels, gas emissions from industrial processes, motor vehicles, and fires are the main sources of air pollution. These sources emit a series of compounds such as particulate matter (PM), sulfur dioxide (SO_2), hydrocarbon (HC), nitrogen oxides (NO_x), ammonia, and volatile organic compounds (VOC) into the atmosphere (de Miranda et al., 2012). These substances, which undergo chemical reactions, dissipate, dilute, and solidify in very complex conditions with others in the atmosphere, are synergistic factors that intensify air pollution.

The rapid increase in the number of vehicles used worldwide is the indicator of the magnitude of the contribution of vehicle traffic to air pollution. Emissions from vehicle traffic are classified as exhaust emission dependent and non-exhaust emissions (Denier van der Gon et al., 2013). Over the past 40 years, while exhaust emissions have been constantly decreasing with legal regulations such as improved exhaust gas treatment and filter technologies, the percentage of non-exhaust emissions has increased due to the increase in the number of vehicles (zum Hagen, Mathissen, Grabiec, Hennicke, Rettig, Grochowicz, Vogt, & Benter, 2019). Non-exhaust emissions that result from vehicle traffic (NEE) refers to particles released into the air due to brake wear, tire wear, road surface wear and resuspension of road dust during vehicle use (Lewis, Moller, & Carslaw, 2019). In urban environments and especially in areas with heavy traffic, a significant amount of the non-exhaust PM is caused by car brakes (Harrison et al., 2012; Thorpe & Harrison, 2008). Reducing car brake particle emissions is an important European Union environmental protection strategy (Perricone et al., 2017).

In a friction brake system in vehicles, friction occurs when the pad and disc pair come into contact. Thus, the rotor slows down or stops. The heat and brake particles formed in braking are released into the atmosphere. High temperature and friction energy are produced during braking. Brake system elements are required to remove this high heat energy from the system quickly. Lamellar graphite cast irons are popular materials in this field due to their high thermal conductivity properties (Yamabe, Takagi, Matsui, Kimura, & Sasaki, 2003). However, in some cases, composites such as aluminum, ceramic matrix composites, and reinforced carbon-carbon elements are also preferred (Güney, Mutlu & Gayretli, 2016; Güney & Mutlu, 2017; Güney & Mutlu, 2019a; Mutlu, Güney, & Erkurt, 2020; Öz, Gürbüz, Yakut, & Sağiroğlu, 2017; Öz et al., 2013).

Motor vehicle brake pads are composites that are made from more than 3000 components, including friction additives held together by binders such as friction materials, reinforcing fibers, filling materials, and phenolic resins (Filip, Kovarik, & Wright, 1997). As the pads are predominantly produced from organic materials, they deteriorate at high temperatures and begin to emit gas and particles to the environment (Chan & Stachowiak, 2004; I. Mutlu, Eldogan & Findik, 2005; Österle, Prietzel, Kloß, & Dmitriev, 2010). This deterioration of organic components causes emissions of very fine amorphous carbon particles and volatile organic compounds (Kukutschová et al., 2011; Plachá et al., 2017).

Passenger cars usually have three different types of pads: non-asbestos organic (NAO), semi-metallic and low metallic. NAO type pads are relatively soft and have lower braking noise compared to other types of pads, but they lose their braking capacity at high temperatures and generate more dust than other types. Although brake pads were made from asbestos fibers for many years, today, asbestos is not used due to serious health problems (Liew &Nirmal, 2013). Airborne PM has a wide range of particle sizes from a few nanometers (nm) diameter to approximately 100 micrometers (μm). Particulate matter from vehicles is usually defined as $PM_{2.5}$ and PM_{10}, depending on the particle size. $PM_{2.5}$ defines particulate matter with less than 2.5 μm of aerodynamic diameter; PM_{10} defines particulate matter with less than 10 μm of aerodynamic diameter (Gehrig et al., 2004).

Non-exhaust emissions mostly contain PM_{10}, but a significant portion of the emissions also include fine $PM_{2.5}$. The chemical properties of non-exhaust PM emissions differ depending on the formulation of the disc/pad pair used, but they mainly contain heavy metals like zinc (Zn), copper (Cu), iron (Fe), nickel (Ni), chrome (Cr) and lead (Pb) (Thorpe & Harrison, 2008). These emissions are chemical components that contribute significantly to negative health effects (Denier van der Gon et al., 2013). The contribution of difference in brake pad composition to emissions is much more than the contribution of the disc or other elements (Pant & Harrison, 2013).

Braking is a quite complicated process. Different amounts of gas are emitted depending on the speed, weight, and deceleration levels; and the pressure and temperature induced accordingly. Different oxidation mechanisms can occur or brake materials can be worn naturally. Adhesive, abrasive, fatigue, and oxidative wear mechanisms are observed at high temperatures. At the end of the process, different amounts of ultra-fine and fine particles are released into the atmosphere (Kukutschová et al., 2009). Mechanical wear occurs at low temperatures. Mechanical wear mainly leads to the emission of coarser particles that belong to the PM_{10} or $PM_{2.5}$ fractions. These particles usually have sharper edges and irregular morphology (Kukutschová et al., 2011). As a result, approximately

40-50% of brake wear is released into the air (zum Hagen, Mathissen, Grabiec, Hennicke, Rettig, Grochowicz, Vogt, Benter, et al., 2019). When the brake system is activated, brake pads apply pressure against the rotors to slow down the vehicle and this results in brake wear and PM formation. The shape, size, and emission rates of brake wear depend on several factors, such as the thermomechanical properties of the rotor, pad, and brake pads. The size of PMs produced by brake wear may be airborne due to local turbulence etc. The release of these toxic particles into the environment may differ in large cities, especially during rush hours when braking is high, due to the frequency of stopping and starting of a large number of vehicles and turbulence of the air (Wahid, 2018).

The nature of the braking process, high energy conditions, and complex metallurgical interactions on the friction surface during braking make it difficult to predict the chemistry and particle size of newly formed species. Even if the raw materials selected for the production of brake pads comply with the emission laws, it is always possible for the newly formed wear particles to have different chemistry and structure (Filip, Weiss, & Rafaja, 2002; Kukutschová et al., 2009). Similarly, the friction performance depends on the wear temperature of the brake materials, the sliding speed, the pressure applied, the chemistry, the structure of the friction pair and the surrounding environment. For example, wear increases as temperature increases (Peter, 2013).

Automotive brake wear, reduction of particle emissions, contribution to environmental pollution and its impact on health have extensively been dealt with in recent years (Joo, Jara, Seo, & Jang, 2020; Lyu, Leonardi, Wahlström, Gialanella, & Olofsson, 2020; Mathissen, Grigoratos, Lahde, & Vogt, 2019; Nosko, Alemani, & Olofsson, 2017; Perricone, Alemani, Wahlström, & Olofsson, 2020; zum Hagen, Mathissen, Grabiec, Hennicke, Rettig, Grochowicz, Vogt, & Benter, 2019). However, very few studies have been found on microstructure characterization. For this purpose, microstructure and chemical properties of the wear particles of the brake discs and pads of vehicles in Turkey were investigated. In the study, the characterization of PM was analyzed using field scanning electron microscopy (SEM), energy dispersing spectrometer (EDS), X-ray diffraction (XRD) and Fourier-transform infrared spectroscopy (FTIR) device.

2. Material and Method

2.1. Brake Wear PM collection

Braking performance was carried out in about 14 hours of structural integrity with a total of 9 steps and 312 braking cycles that included instrument check stop (23 repetitions), burnish (200 repetitions), effectiveness (16 repetitions), fade (15 repetitions), hot performance (2 repetitions), cooling (4 repetitions), recovery ramp (2 repetitions), reburnish (35 repetitions), and final effectiveness (15 repetitions). The wear residue that formed during the braking test was aspirated to the particle collection unit shown in Figure 1 and accumulated in an atmospheric environment. It was preserved in a glass bottle for laboratory tests.

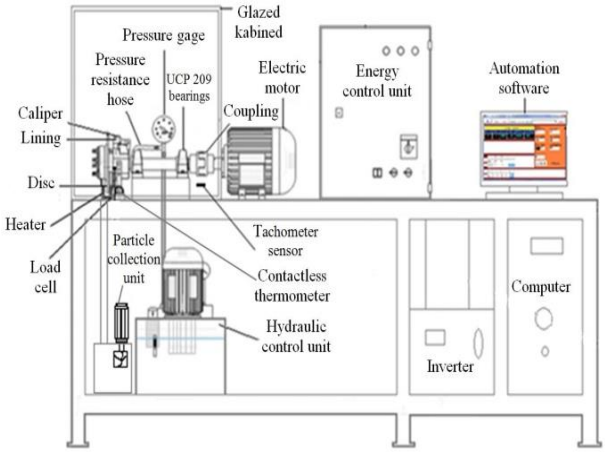

Fig 1.Schematic representation of the braking test device and particle collection unit (Güney & Mutlu, 2019a)

2.2 Chemical Characterization

Microstructure analysis was performed in the SEM (HITACHI SU5000) device equipped with EDS in Material Characterization Laboratory of Karamanoğlu Mehmetbey University, Scientific and Technological Research Application and Research Center. In order to understand brake wear crystal forms, a Bruker D8 enhanced diffractometer (λ = 1.5406 Å) with X-ray diffraction (XRD) Cu-Ka radiation was used**.** IR spectroscopy (Bruker Vertex 70 ATR) was used to measure the FTIR spectrum of the sample. The data were collected by vibration frequencies at 4000-400 cm^{-1}scanning range at 4 cm^{-1}spectral resolution.

3. Results and Discussion

3.1 Characterization by SEM and EDS

Brake wear and particle emission rates are greatly affected by the chemical composition of the brake pads or brake discs and the driving mode. Table 1 shows the elemental composition of the cast-iron disc used for braking. In semi-metallic friction materials, mostly metals such as Fe and Cu and other additives contribute to particle emission. In braking, 90% of total wear occurs on pads (Sanders, Xu, Dalka, Maricq, 2003)**.**

Table1.The chemical composition of the disc (Güney & Mutlu, 2019b)

Elements	Fe	C	Si	Mn	P	S	Cr	Mo	Ni	Al	Cu	Ag	Ti	V	Mg	Zr
Weight %	93.56	3.61	1.81	0.586	0.025	0.023	0.116	0.021	0.033	-	0.005	-	0.015	-	0.003	-

The size distributions and morphology of the wear residue particles formed during the 14 hour period, 9 steps, and 312 braking cycles were analyzed. In Figure 2 (a), (b), (c), and (d), the condensed amorphous agglomerated formations of wear particles are shown by SEM micrographs at different magnifications. The size distribution of the wear particles in the air produced during braking varies depending on the time since the start of the test. During braking, particle structure is affected by factors such as pressure, speed, and temperature. In cases where the rotor is relatively cold, nano-sized ultra-fine particles are produced. In cases where the rotor temperature increases, the shape of particle size distributions and their changes over time appear to be formed by the agglomeration of submicron particles, then primary nanoparticles in the evaporation/condensation process (Kukutschová et al., 2009).

During the braking cycle, the temperature varied between 100-400 ^{0}C r (Güney, Mutlu & Gayretli, 2016; Güney & Mutlu, 2017; Güney & Mutlu, 2019a; Mutlu, Güney, & Erkurt, 2020). It is seen in the micrographs that the particles are agglomerated by forming groups. This agglomeration occurs in different chemical and metallurgical bonds, partly due to condensation. Besides, high-speed friction is caused by the kinetic energy charging the particles. The micrograph in Figure 2 (a)shows that the cloud-shaped gray nano-particles agglomerate to form predominantly oxidized structures. The concentration of agglomerated particles shown in the micrograph is less than 1 μm. The temperature of the disc surface rises to 380 ^{0}C during braking. As the particle bonding forces will decrease with the effect of heat, the number of particles increases as the temperature increases (Garg et al., 2000). The micrograph is given in Figure 2 (b) shows that the agglomerated particle size is 2-3 μm. Figure 2 (c) shows that particle size distributions differ under different braking conditions. In the micrograph of Figure 2 (d), it can be easily seen that particles larger than 1 μm decrease, and nano-sized particles increase significantly due to the high temperature in braking. The grain particulate matter consists of larger isolated particles as well as smaller particles that tend to accumulate. This tendency occurs through the evaporation/condensation/agglomeration of organic components of the friction composite. Besides, we see that the wear particles are ground to nanoscale levels during the abrasive wear mechanism. The micrograph shows that the primary particles are about 10 nm in size. The oxidative character of friction operations during braking also promotes this situation (Kukutschová et al., 2011). It was confirmed by SEM analysis that some of the abrasion particles analyzed in the study were PM_{10} and most of them were $PM_{2.5}$ class particulate matter.

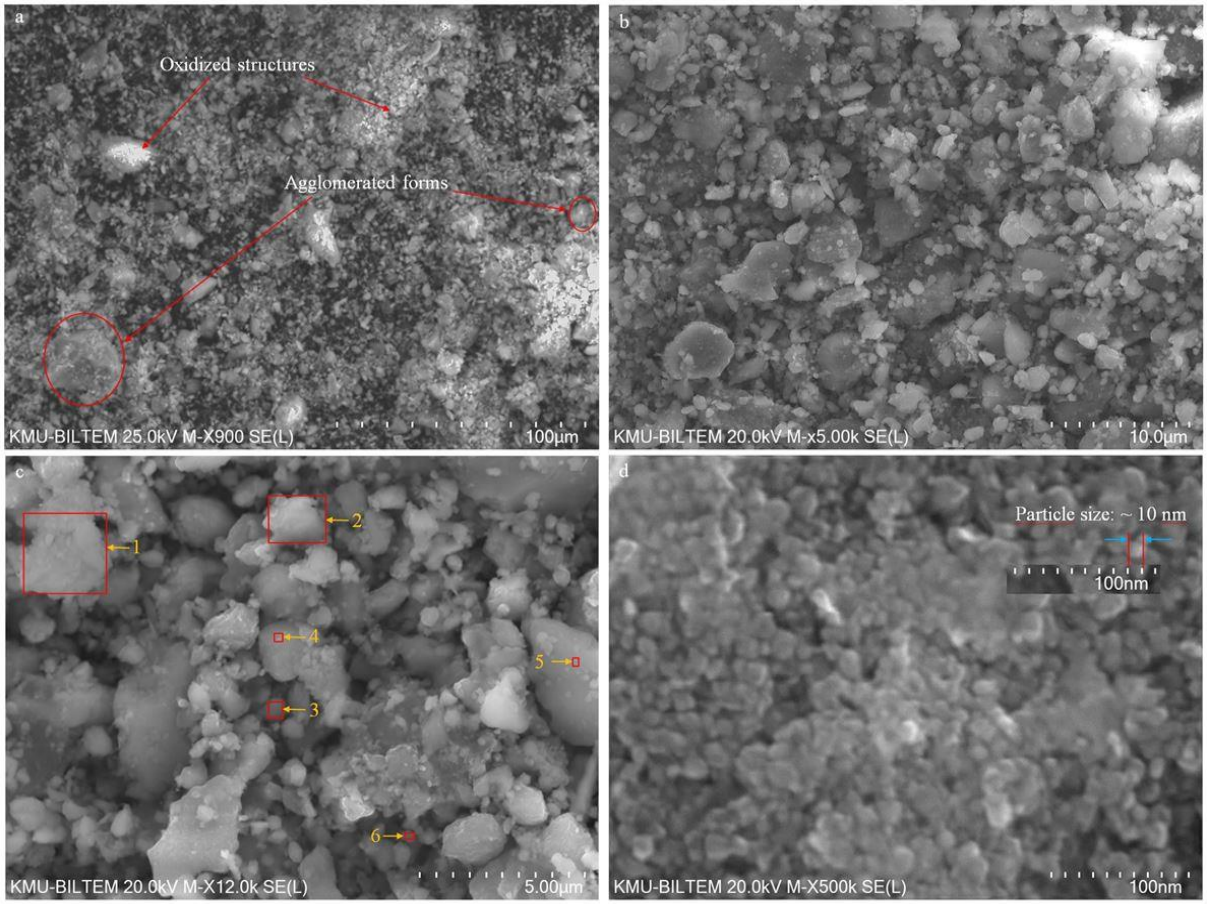

Fig 2**.** SEM images of brake wear particles; (a) 900 X magnification, (b) 5.00 kX magnification, (c) 12.0 kX magnification, (d) 500 kX magnification

Table 2. Atomic amounts of elements detected by EDS analysis

	Fig 2. (a)	Fig 2. (c)					
Elements	surface atomic %	1.point atomic %	2. point atomic %	3. point atomic %	4. point atomic %	5. point atomic %	6. point atomic %
C	4,59	6,83	3,19	7,49		3,96	3,16
N	1,49	1,53	1,13	2,01	1,63	1,83	1,27
O	51,53	56,36	57,48	61,39	60,53	61,42	43,48
F	4,52	4,71	4	3,75	4,44	9,01	7,59
Mg	0,67	0,99	0,67	0,41	0,71	0,47	0,41
Br	0,47	0,58	0,43	0,43	0,49	0,49	0,88
Al	0,59	0,6	0,81		0,84	0,36	0,86
Si	3,77	4	4,94	1,69	4,76	2,44	2,6
P	0,34	0,39	0,25	0,34	0,44	0,58	0,63
Zr				0,01		0,01	
Nb			0,01				
Mo	0,06	0,05		0,03	0,03	0,01	0,1
S	0,27	0,29	0,34	0,17	0,25	0,28	0,34
Cl	0,08	0,08	0,09	0,06	0,06	0,06	0,07
K	0,26	0,29	0,33	0,09	0,42	0,19	0,3
Ca	6,1	5,41	5,42	14,74	5,82	1,66	1,97
Sc	0,09	0,12	0,11	0,18	0,11	0,05	0,09
Ti	0,05	0,05	0,08				0,05
V	0,04	0,04	0,04			0,03	0,07
Cr	0,04	0,09	0,08	0,03	0,06	0,04	0,13
Mn	0,11	0,11	0,13	0,06	0,11	0,12	0,2
Fe	16,02	16,33	19,11	6,21	17,37	15,46	32,63
Co	0,38	0,37	0,44	0,13	0,47	0,49	0,92
Ni		0,07			0,05	0,07	0,15
Cu	1,4	0,41	0,5	0,15	0,44	0,42	1,15
Zn	0,07	0,07	0,09	0,03	0,09	0,07	0,2
Se	0,16	0,15	0,13	0,09	0,09	0,1	0,39

Garg et al. (2000) reported that an average of 35% of vehicle brake pad mass loss spread to the air as PM (<100 μm), and 63% of PM in the air was smaller than 10 μm to 2.5 μm in diameter (Garg et al., 2000). Sanders et al. (2003) concluded that approximately 50% of brake wear particles spread as airborne matter in braking tests. As it is understood from the comparison with the micrograph scale by the literature, the number of wear particles smaller than 500 nm is much more than the number of particles larger than 1 μm. t is generally known that particle size determines the effects on health as well as structure, surface area, and chemical composition (Geiser, & Kreyling, 2010).

Surface, regional, and point EDS analyzes of micrographs in Figure 2 are provided in Table 2. The data in Table 2 show that the elemental composition of all fractions collected by aspirating during braking is consistent with the literature (Afiqah, Fauziana, Rasid, & Wong, 2015; Hulskotte, Roskam, & Van Der Gon, 2014; Kennedy & Gadd, 2003). In all analyzes, C, N, O, F, Si, Ca, Fe and Cu elements are atomically dominant. The dominant metallic elements are Fe (atomic up to 32.63%), followed by Si (atomic up to 4.94%), and Cu (atomic up to 1.15%). The other elements Mg, Br, Al, S, P, Zr, Nb, Mo, S, Cl, K, Sc, Ti, V, Cr, Mn, Co, Ni, Zn, and S are present in PM composition in atomically lower levels. This may be related to the fact that oxidation of all metals and Cu, Zn, and Sn can be easier to break down (making nanoparticles) than steel and cast iron due to lower mechanical properties (yield stress, strength). Besides, lower melting points of Cu, Zn, and Sn compared to Fe/steel may cause easier nanoparticle formation. On the other hand, higher Fe content in larger particle fractions was due to the high amount in disc material structure. All detected elements appear depending on the chemical structure of the disc/pad materials under different braking conditions. Also, it is possible for elements found in high amounts in the atmosphere such as N and O to get involved in the structure in different forms with various reactions due to the high temperature in braking.

3. 2 Characterization by XRD

The XRD analysis on wear residues is an important technique for confirming chemical data on the composition of the disc/pad pair (Verma et al., 2015). Because this technique provides information about structural transformations that occur under specific wear mechanisms under different test conditions. Figure 3 shows the X-ray diffraction pattern of the vacuum collected abrasions in the braking test with commercial disc/pad material in the test device with a 312 braking cycle. The main phases are oxide phases such as Fe_3O_4, MgO, Al_2O_3, CuO, SO_3, CaO, K_2O, SiO_2, MnO_2, Cr_2O_3, $ZrSiO_4$, Ca_2SiO_4, TiO_2, ZnO, Fe, Fe_2O_3. This data is a clear indication that the wear particles produced by the braking mechanism carried out under different conditions may have very different phase compositions. The results of the analysis show that iron oxides such as FeO and Fe_3O_4 and Fe_2O_3, which result from the tribo-oxidation of the cast-iron disc in highly oxidative environments, exist predominantly in the structure, following the literature results (Aku, Yawas, Madakson, & Amaren, 2012; Giovanni Straffelini & Molinari, 2011; Straffelini, Pellizzari, & Maines, 2011; Verma et al., 2015) for such tribological systems. All oxides are largely present in the structure depending on the reaction mechanism of the abrasions with the outer atmosphere. Phase structures of forms compatible with XRD spectra are given in Table 3.

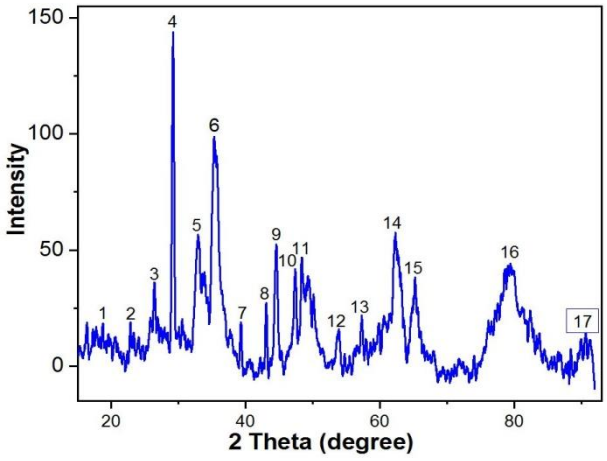

Fig 3. Typical XRD pattern of brake wear particles

Table 3. XRD diffraction spectrum peak numbers of brake wear particles

Name	Formula	Crystal system	Peak number
Ethane	$C_{10}H_{12}O_4$	Tetragonal	1, 2, 3
Chegemite (mineral)	$C_7(SiO_4)_3(OH)_2$	Orthorhombic	5, 6, 10, 11
NitroquanylAzide	$CH_2N_6O_2$	Triclinic	3, 4, 5, 7
Calcium Silicon Oxide	Ca_2SiO_4	Triclinic	5, 6
Thione	$C_7H_5N_3S_2$	Monoclinic	3, 4
Calcium Iron Oxide	$Ca_2Fe_{15}51O_{25}$	Orthorhombic	3, 4, 5, 6
Guanine Hydrochloride Hydrate	$C_5H_5N_5O$ HCL H_2O	Monoclinic	2, 3, 4, 6
Glycine Phosphate	$C_2H_8NO_5P$	Monoclinic	3, 4, 6, 11
Oxamide	$C_2H_4N_2O_2$		1, 2, 3, 4, 6, 12, 14
Methyl Sulfide	$S_2(CH_3)_2$	Monoclinic	3, 5, 6
Silicon Boride	SiB_3	Orthorhombic	3, 4, 6, 9, 10, 11
Nickel Vanadium Oxide Hydrate	$Ni(V_2O_6)(H_2O)$	Triclinic	1, 2, 3, 4, 5
Iron Oxide	FeO	Cubic	6, 13, 16
Cohenite	Fe_3C	Orthorhombic	8, 9, 10, 11, 16, 17
Hematite	Fe_2O_3	Rhombohedral	5, 6, 8, 12, 13, 14, 15, 16, 17
Magnetite	Fe_3O_4	Orthorhombic	3, 6, 8, 14, 17
Calcium Boron Carbide Chloride	$Ca_9Cl_8(BC_2)_2$	Orthorhombic	3, 5, 9, 10
Aluminum Hydrogen Phosphate	$Al_2(HPO_3)_3$	Hexagonal	3, 4, 6
Nickel Iron Vanadium Oxide	Ni_2FeVO_6	Orthorhombic	6
Zinc Vanadium Oxide	Zn V_3O_8	Orthorhombic	1, 2, 4, 2, 11, 13
Calcium Oxide	CaO	Cubic	5, 6
Calcite	$CaCO_3$	Rhombohedral	4, 6, 7, 8, 10, 11, 12, 13, 15, 16
Copper Iron Oxide	$Cu(Fe_2O_4)$	Cubic	3, 4, 5, 8, 9, 10, 11
Copper Aluminum Sulfite	$CuAlS_2$	Tetragonal	4, 11, 13, 16
Tin Niobium Oxide	$Sn_2(Nb_2O_7)$	Cubic	4, 5, 11, 13, 16, 17
Aluminum Oxide	Al_2O_3	Hexagonal	5, 6, 9, 10, 11, 13, 14, 16
Calcium Aluminum Oxide	$CaAl_2O_4$	Monoclinic	6, 9,10
Poly-p-xylylene	$(C_8H_8)_n$	Monoclinic	1, 2, 3, 6, 9, 11,
Carbon Oxide	CO_2	Cubic	3, 6, 7, 9, 10
Copper Oxide	CuO	Monoclinic	6, 9, 11, 15, 16
Magnesıum Oxide	MgO	Hexagonal	4, 8, 14, 16
Manganese Oxide	MnO_2	Hexagonal	4, 5, 6, 9, 13, 15
Hausmannite	Mn_3O_4	Tetragonal	4, 5, 6, 9, 12, 13, 15
Manganese Silicon	MnSi	Cubic	5, 9, 10, 16
Nitrogen Oxide	N_2O_2	Monoclinic	1, 3, 4, 5, 6, 9, 13
Sulfur Oxide	SO_3	Orthorhombic	2
Silicon Oxide	SiO_2	Hexagonal	3, 4, 11
Silicon Carbide	SiC		5, 6, 13
Chromium Oxide	Cr_2O_3	Rhombohedral	5
Potassium Oxide	K_2O	Hexagonal	3, 10
Zirconium Silicon Oxide	$ZrSiO_4$		5, 6
Titanium Oxide	TiO_2	Cubic	4, 12
Zinc Oxide	ZnO	Hexagonal	14, 15
Nickel Oxide	NiO_2	Hexagonal	6, 9, 15

3. 3 Characterization by FTIR

Brake wear particulate matter (PM) is a complex mixture of many different elements. But it is possible to determine the amount of more than one species by FTIR (Fourier-transform infrared) spectroscopy. We can determine more than one bond structure by interpreting the spectra obtained. Nevertheless, the absorption peaks overlapping with the condensed phase spectrum of PM are very difficult to identify as they cause scattering into a very wide and mid-infrared spectrum. However, bond structures are determined using standards created for the estimation of inorganic substances or organic functional groups. Per the EDS results of PM, the bond structures of the existing elements in the structure were determined. According to the peak values shown in Figure 4; the peaks in the 3691, 1795 cm^{-1} band range show O-H stresses in the structure. This indicates the presence of the H_2O molecule. The peaks of O-C stresses in the range of 1415, 1620, 1795, 2156, 2509, 2854, 2935, 3309, and 3691 cm^{-1}indicate the presence of CO_2 molecules in the structure. The peaks between 2156, 1620 cm^{-1} indicate the presence of CO molecules. The peaks of H-C stresses in the range of 436, 521, 708, 798,872, 1012, 1415, 1620, 1795, 2156 cm^{-1} indicate the presence of HC molecules. he temperatures rise to 400 ^{0}C during braking. It was confirmed by XRD models that hydrocarbon (HC) emissions occur at these temperatures. The peaks of S-O stresses between 1415 and 1012 cm^{-1} indicate the presence of SO_2 molecule in the structure. The peaks of N-O stresses in the range of 1012, 872, 798, and 708 cm^{-1} show that NO_x free and mixed bonded molecules exist in the structure. It shows that oxide bonds in different structures between 1012 and 436 cm^{-1} bands may exist due to the stretching of oxide bonds. Because oxides often exhibit peaks below 1000 cm^{-1}, which may be caused by inter-atomic vibrations (Boroń et al., 2019).

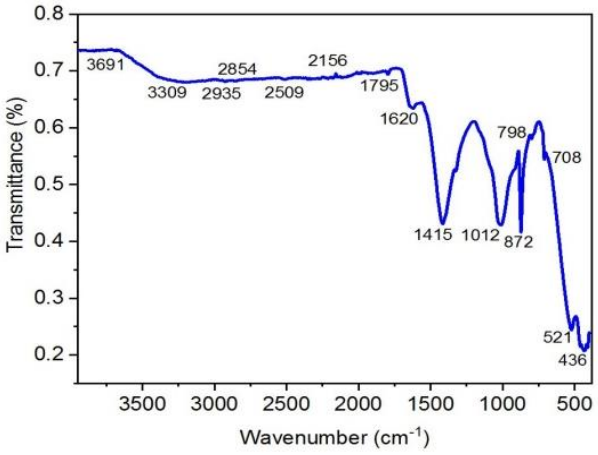

Fig 4. FTIR spectrum of brake wear particles

Brake wear particles have a rich chemical composition. During braking, a certain amount of this rich structure form wears by abrasion, burning, or evaporation. Brake wears contain very different structures by nature. Therefore; 1415, 1620, 1795, 2156, 2509, 2854, 2935, 3309 and 3691 cm^{-1} peak points obtained from FTIR analysis were caused by stretching the bonds of Al-O**,** Br-O, Ca-O, Cl-O, C-O, CO, CH_4, C_2H_2,H-C, C-C, C-F, C-Br, Co-O, Cr-O, Cu-O, N-H, C-N, Fe-O**,** Fe_2O_4**,** F_2O_3**,** K-O, F-O, Mg-O, Mn-O**,** Mo-O, N-O, Nb-O, Ni-O, P-O, S-O, Sc-O, Si-O**,** Ti-O, V-O, Zn-O, Zr-O functional groups. When FTIR measurements were evaluated, it was concluded that there are molecular bond structures equivalent to elemental structures determined by EDS analysis. In addition, the existence of bond structures compatible with crystal structures detected by XRD analysis was agreed on.

The elements and crystal structures in the chemical structure of PM analyzed in the study spread over a wide range. How and from which source these combinations are incorporated into the structure is beyond the scope of this study.

4. Conclusions and Recommendations

Important points of this study on microstructure and chemical characterization of total non-exhaust PM emissions can be emphasized as follows: Brake wear particles constitute a significant part of non-exhaust emissions. The elemental composition of the analyzed OEM disc/pad pair significantly determined the emission substances they emit. Metals and heavy metals in the composition are released into the environment as emissions, which can have significant toxic effects. t was determined by SEM analysis that ultrafine primary brake wear grains formed larger grains by agglomerating through reactions such as condensation/evaporation. n addition, brake wear primary particles were generally detected in less than 1 μm and greater than 10 nm ultra-fine grain sizes. The most important chemical components of the brake wear were determined as C, O, Fe, and Cu by EDS analysis. High levels of Fe, C, and O were attributed to the significant spread of oxidized crystals and pollutant structures such as Fe_2O_3, Fe_3O_4 to the environment. Oxide, sulfate, phosphate, and different mineral structures produced by brake wear were determined by XRD analysis. Also, it was determined by FTIR analysis that important emission substances such as HC, NO, CO, SO and organic compounds spread to the environment through brake wear. Most fractions of brake wear contain respirable particles.Therefore, some components of brake wear particles in the air have been considered as potential hazards to environmental safety and human health. In the future, studies can be conducted on the negative effects of brake wear particle chemical components on environmental safety and human health.

References

1. Amato, F. (Ed.). (2018). *Non-exhaust emissions: an urban air quality problem for public health; impact and mitigation measures*. Academic Press.
2. Khodakarami, J., & Ghobadi, P. (2016). Urban pollution and solar radiation impacts. *Renewable and Sustainable Energy Reviews*, *57*, 965-976.
3. Pope Iii, C. A., Burnett, R. T., Thun, M. J., Calle, E. E., Krewski, D., Ito, K., & Thurston, G. D. (2002). Lung cancer, cardiopulmonary mortality, and long-term exposure to fine particulate air pollution. *Jama*, *287*(9), 1132-1141.
4. Oberdörster, G., Maynard, A., Donaldson, K., Castranova, V., Fitzpatrick, J., Ausman, K., ... & Olin, S. (2005). Principles for characterizing the potential human health effects from exposure to nanomaterials: elements of a screening strategy. *Particle and fiber toxicology*, *2*(1), 8.
5. Radhakrishnan, S., Devarajan, Y., Mahalingam, A., & Nagappan, B. (2017). Emissions analysis on a diesel engine fueled with palm oil biodiesel and pentanol blends. *Journal of Oil Palm Research*, *29*(3), 380-386.
6. de Miranda, R. M., de Fatima Andrade, M., Fornaro, A., Astolfo, R., de Andre, P. A., & Saldiva, P. (2012). Urban air pollution: a representative survey of PM 2.5 mass concentrations in six Brazilian cities. *Air Quality, Atmosphere & Health*, *5*(1), 63-77.

7. Denier van der Gon, H. A., Gerlofs-Nijland, M. E., Gehrig, R., Gustafsson, M., Janssen, N., Harrison, R. M., ... & Krijgsheld, K. (2013). The policy relevance of wear emissions from road transport, now and in the future—an international workshop report and consensus statement. *Journal of the Air & Waste Management Association*, *63*(2), 136-149.
8. zum Hagen, F. H. F., Mathissen, M., Grabiec, T., Hennicke, T., Rettig, M., Grochowicz, J., ... & Benter, T. (2019). On-road vehicle measurements of brake wear particle emissions. *Atmospheric Environment*, *217*, 116943.
9. Lewis, A., Moller, S. J., & Carslaw, D. (2019). Non-Exhaust Emissions from Road Traffic.
10. Thorpe, A., & Harrison, R. M. (2008). Sources and properties of non-exhaust particulate matter from road traffic: a review. *Science of the total environment*, *400*(1-3), 270-282.
11. Harrison, R. M., Jones, A. M., Gietl, J., Yin, J., & Green, D. C. (2012). Estimation of the contributions of brake dust, tire wear, and resuspension to nonexhaust traffic particles derived from atmospheric measurements. *Environmental science & technology*, *46*(12), 6523-6529.
12. Perricone, G., Alemani, M., Metinöz, I., Matějka, V., Wahlström, J., & Olofsson, U. (2017). Towards the ranking of airborne particle emissions from car brakes–a system approach. *Proceedings of the Institution of Mechanical Engineers, Part D: Journal of Automobile Engineering*, *231*(6), 781-797.
13. Yamabe, J., Takagi, M., Matsui, T., Kimura, T., & Sasaki, M. (2003). Development of disc brake rotors for heavy-and medium-duty trucks with high thermal fatigue strength. *SAE transactions*, 124-131.
14. Güney, B., & Mutlu, I. (2019). TRIBOLOGICAL PROPERTIES OF BRAKE DISCS COATED WITH Cr2O3–40% TiO2 BY PLASMA SPRAYING. *Surface Review and Letters*, *26*(10), 1950075.
15. Guney, B., Mutlu, I., & Gayretli, A. (2016). Investigation of braking performance of NiCrBSi coated brake discs by flame spraying. *Journal of the Balkan Tribological Association*, *22*(1 A), 887-903.
16. Güney, B., & Mutlu, İ. (2017). Dry friction behavior of NiCrBSi-% 35W2C coated brake disks. *Materials Testing*, *59*(5), 497-505.
17. Mutlu, İ., Güney, B., & Erkurt, İ. Investigation of the effect of Cr2O3-2% TiO2 coating on braking performance. *International Journal of Automotive Engineering and Technologies*, *9*(1), 29-41.
18. Öz, A., Gürbüz, H., Yakut, A. K., & Sağiroğlu, S. (2017). Braking performance and noise in excessively worn brake discs coated with HVOF thermal spray process. *Journal of Mechanical Science and Technology*, *31*(2), 535-543.
19. Öz, A., Samur, R., Mindivan, H., Demir, A., Sagiroglu, S., & Yakut, A. K. (2013). Effect of heat treatment on the wear and corrosion behaviors of a gray cast iron coated with a COLMONOY 88 alloy deposited by high velocity oxygen fuel (HVOF) thermal spray. *Metalurgija*, *52*(3), 368-370.
20. Filip, P., Kovarik, L., & Wright, M. A. (1997). *Automotive brake lining characterization* (No. 973024). SAE Technical Paper.
21. Österle, W., Prietzel, C., Kloß, H., & Dmitriev, A. I. (2010). On the role of copper in brake friction materials. *Tribology International*, *43*(12), 2317-2326.
22. Chan, D. S. E. A., & Stachowiak, G. W. (2004). Review of automotive brake friction materials. *Proceedings of the Institution of Mechanical Engineers, Part D: Journal of Automobile Engineering*, *218*(9), 953-966.
23. Mutlu, I., Eldogan, O., & Findik, F. (2005). Production of ceramic additive automotive brake lining and investigation of its braking characterisation. *Industrial Lubrication and Tribology*.
24. Kukutschová, J., Moravec, P., Tomášek, V., Matějka, V., Smolík, J., Schwarz, J., ... & Filip, P. (2011). On airborne nano/micro-sized wear particles released from low-metallic automotive brakes. *Environmental Pollution*, *159*(4), 998-1006.
25. Plachá, D., Vaculík, M., Mikeska, M., Dutko, O., Peikertová, P., Kukutschová, J., ... & Filip, P. (2017). Release of volatile organic compounds by oxidative wear of automotive friction materials. *Wear*, *376*, 705-716.
26. Liew, K. W., & Nirmal, U. (2013). Frictional performance evaluation of newly designed brake pad materials. *Materials & Design*, *48*, 25-33.
27. Gehrig, R., Hill, M., Buchmann, B., Imhof, D., Weingartner, E., & Baltensperger, U. (2004). Separate determination of PM10 emission factors of road traffic for tailpipe emissions and emissions from abrasion and resuspension processes. *International Journal of Environment and Pollution*, *22*(3), 312-325.
28. Pant, P., & Harrison, R. M. (2013). Estimation of the contribution of road traffic emissions to particulate matter concentrations from field measurements: a review. *Atmospheric environment*, *77*, 78-97.
29. Kukutschová, J., Roubíček, V., Malachová, K., Pavlíčková, Z., Holuša, R., Kubačková, J., ... & Filip, P. (2009). Wear mechanism in automotive brake materials, wear debris and its potential environmental impact. *Wear*, *267*(5-8), 807-817.
30. zum Hagen, F. H. F., Mathissen, M., Grabiec, T., Hennicke, T., Rettig, M., Grochowicz, J., ... & Benter, T. (2019). Study of brake wear particle emissions: impact of braking and cruising conditions. *Environmental science & technology*, *53*(9), 5143-5150.
31. Wahid, S. M. (2018). Automotive brake wear: a review. *Environmental Science and Pollution Research*, *25*(1), 174-180.
32. Filip, P., Weiss, Z., & Rafaja, D. (2002). On friction layer formation in polymer matrix composite materials for brake applications. *Wear*, *252*(3-4), 189-198.
33. Peter, F. (2013). Friction brakes for automotive and aircraft. In *Encyclopedia of tribology* (pp. 1296-1304). Springer US.
34. Joo, B. S., Jara, D. C., Seo, H. J., & Jang, H. (2020). Influences of the average molecular weight of phenolic resin and potassium titanate morphology on particulate emissions from brake. *Wear*, 203243.
35. Lyu, Y., Leonardi, M., Wahlström, J., Gialanella, S., & Olofsson, U. (2020). Friction, wear and airborne particle emission from Cu-free brake materials. *Tribology International*, *141*, 105959.
36. Nosko, O., Alemani, M., & Olofsson, U. (2017). Characterisation of airborne particles emitted from car brake materials. In *Proc. 6th World Tribology Congress, September* (pp. 17-22).
37. Mathissen, M., Grigoratos, T., Lahde, T., & Vogt, R. (2019). Brake wear particle emissions of a passenger car measured on a chassis dynamometer. *Atmosphere*, *10*(9), 556.

38. Perricone, G., Alemani, M., Wahlström, J., & Olofsson, U. (2020). A proposed driving cycle for brake emissions investigation for test stand. *Proceedings of the Institution of Mechanical Engineers, Part D: Journal of Automobile Engineering*, *234*(1), 122-135.
39. Sanders, P. G., Xu, N., Dalka, T. M., & Maricq, M. M. (2003). Airborne brake wear debris: size distributions, composition, and a comparison of dynamometer and vehicle tests. *Environmental science & technology*, *37*(18), 4060-4069.
40. Güney, B., & Mutlu, I. (2019). Wear and corrosion resistance of Cr2O3%-40% TiO2 coating on gray cast-iron by plasma spray technique. *Materials Research Express*, *6*(9), 096577.
41. Garg, B. D., Cadle, S. H., Mulawa, P. A., Groblicki, P. J., Laroo, C., & Parr, G. A. (2000). Brake wear particulate matter emissions. *Environmental Science & Technology*, *34*(21), 4463-4469.
42. Geiser, M., & Kreyling, W. G. (2010). Deposition and biokinetics of inhaled nanoparticles. *Particle and fibre toxicology*, *7*(1), 2.
43. Hulskotte, J. H. J., Roskam, G. D., & Van Der Gon, H. D. (2014). Elemental composition of current automotive braking materials and derived air emission factors. *Atmospheric environment*, *99*, 436-445.
44. Afiqah, O., Fauziana, I., Rasid, O., & Wong, S. V. (2015). Elemental composition study of commercial brake pads for a passenger vehicle: A case study. *Recent Advances in Mechanics and Mechanical Engineering*.
45. Kennedy, P., & Gadd, J. (2003). Preliminary examination of trace elements in tyres, brake pads, and road bitumen in New Zealand. *Prepared for Ministry of Transport, New Zealand, Infrastructure Auckland*.
46. Verma, P. C., Menapace, L., Bonfanti, A., Ciudin, R., Gialanella, S., & Straffelini, G. (2015). Braking pad-disc system: wear mechanisms and formation of wear fragments. *Wear*, *322*, 251-258.
47. Straffelini, G., Pellizzari, M., & Maines, L. (2011). Effect of sliding speed and contact pressure on the oxidative wear of austempered ductile iron. *Wear*, *270*(9-10), 714-719.
48. Straffelini, G., & Molinari, A. (2011). Mild sliding wear of Fe–0.2% C, Ti–6% Al–4% V and Al-7072: a comparative study. *Tribology letters*, *41*(1), 227-238.
49. Aku, S. Y., Yawas, D. S., Madakson, P. B., & Amaren, S. G. (2012). Characterization of periwinkle shell as asbestos-free brake pad materials. *The Pacific Journal of Science and Technology*, *13*(2), 57-63.
50. Boroń, P., Rutkowska, M., Gil, B., Marszałek, B., Chmielarz, L., & Dzwigaj, S. (2019). Experimental Evidence of the Mechanism of Selective Catalytic Reduction of NO with NH3 over Fe-Containing BEA Zeolites. *ChemSusChem*, *12*(3), 692-705.